

Fisker, Peter Simonsen; Malmgren-Hansen, David; Sohnesen, Thomas Pave

**Working Paper**

## Remote sensing of urban cyclone impact and resilience: Evidence from Idai

WIDER Working Paper, No. 2021/89

**Provided in Cooperation with:**

United Nations University (UNU), World Institute for Development Economics Research (WIDER)

*Suggested Citation:* Fisker, Peter Simonsen; Malmgren-Hansen, David; Sohnesen, Thomas Pave (2021) : Remote sensing of urban cyclone impact and resilience: Evidence from Idai, WIDER Working Paper, No. 2021/89, ISBN 978-92-9267-029-0, The United Nations University World Institute for Development Economics Research (UNU-WIDER), Helsinki, <https://doi.org/10.35188/UNU-WIDER/2021/029-0>

This Version is available at:

<https://hdl.handle.net/10419/243415>

**Standard-Nutzungsbedingungen:**

Die Dokumente auf EconStor dürfen zu eigenen wissenschaftlichen Zwecken und zum Privatgebrauch gespeichert und kopiert werden.

Sie dürfen die Dokumente nicht für öffentliche oder kommerzielle Zwecke vervielfältigen, öffentlich ausstellen, öffentlich zugänglich machen, vertreiben oder anderweitig nutzen.

Sofern die Verfasser die Dokumente unter Open-Content-Lizenzen (insbesondere CC-Lizenzen) zur Verfügung gestellt haben sollten, gelten abweichend von diesen Nutzungsbedingungen die in der dort genannten Lizenz gewährten Nutzungsrechte.

**Terms of use:**

*Documents in EconStor may be saved and copied for your personal and scholarly purposes.*

*You are not to copy documents for public or commercial purposes, to exhibit the documents publicly, to make them publicly available on the internet, or to distribute or otherwise use the documents in public.*

*If the documents have been made available under an Open Content Licence (especially Creative Commons Licences), you may exercise further usage rights as specified in the indicated licence.*



WIDER Working Paper 2021/89

## **Remote sensing of urban cyclone impact and resilience**

Evidence from Idai

Peter Fisker,<sup>1</sup> David Malmgren-Hansen,<sup>2</sup> and Thomas Pave  
Sohnesen<sup>2</sup>

June 2021

**Abstract:** Cyclone Idai, the most devastating cyclone ever recorded in Southern Africa, caused havoc in large parts of central Mozambique, especially the port city of Beira, upon its landfall in March 2019. This study reviews and compares measurements of the impact, using various sources of remote sensing data. Furthermore, taking into account pre-cyclone neighbourhood characteristics and post-cyclone developments in building quantity and quality, it is shown that: i) spatial patterns of severity of impact vary substantially by data source and method used, ii) a small but measurable share of the cross-city variation in cyclone damage can be explained by prior neighbourhood-level characteristics, and finally, iii) a convolutional neural network building detector and classifier applied to a panel of high resolution satellite images fails to prove clear patterns in the post-cyclone rebuilding of Beira up to 17 months after the cyclone. Although the present analysis shows mixed results, and more work validating the various links between satellite data, operational use, and economic analysis is needed, remote sensing may still be the best option in a data-scarce disaster situation.

**Key words:** remote sensing, cyclones, urban, resilience

**JEL classification:** O18, Q54, R11

**Acknowledgements:** The authors would like to thank participants at the 2020 Annual Conference on Inclusive Growth in Mozambique for their valuable comments.

---

<sup>1</sup> Department of Economics, University of Copenhagen, Denmark, corresponding author: [pkf@econ.ku.dk](mailto:pkf@econ.ku.dk); <sup>2</sup> Independent consultant

This study has been prepared within the UNU-WIDER project [Inclusive growth in Mozambique – scaling-up research and capacity](#) implemented in collaboration between UNU-WIDER, University of Copenhagen, University Eduardo Mondlane, and the Mozambican Ministry of Economics and Finance. The project is financed through specific programme contributions by the governments of Denmark, Finland, and Norway.

Copyright © UNU-WIDER 2021

UNU-WIDER employs a fair use policy for reasonable reproduction of UNU-WIDER copyrighted content—such as the reproduction of a table or a figure, and/or text not exceeding 400 words—with due acknowledgement of the original source, without requiring explicit permission from the copyright holder.

Information and requests: [publications@wider.unu.edu](mailto:publications@wider.unu.edu)

ISSN 1798-7237 ISBN 978-92-9267-029-0

<https://doi.org/10.35188/UNU-WIDER/2021/029-0>

Typescript prepared by Siméon Rapin.

United Nations University World Institute for Development Economics Research provides economic analysis and policy advice with the aim of promoting sustainable and equitable development. The Institute began operations in 1985 in Helsinki, Finland, as the first research and training centre of the United Nations University. Today it is a unique blend of think tank, research institute, and UN agency—providing a range of services from policy advice to governments as well as freely available original research.

The Institute is funded through income from an endowment fund with additional contributions to its work programme from Finland, Sweden, and the United Kingdom as well as earmarked contributions for specific projects from a variety of donors.

Katajanokanlaituri 6 B, 00160 Helsinki, Finland

The views expressed in this paper are those of the author(s), and do not necessarily reflect the views of the Institute or the United Nations University, nor the programme/project donors.

## 1 Introduction

On the night between 14 and 15 March 2019, a tropical cyclone by the name of Idai made landfall on the east coast of central Mozambique, causing massive damage to the city of Beira and subsequent flooding of its hinterlands. In the Southern Hemisphere, Idai ranks as one of the most severe storms in history with gusts exceeding 110 km/h in the city of Beira.

As the frequency of tropical cyclones in Eastern Africa is expected to increase as a consequence of climate change, it becomes more and more urgent to study the impacts of weather-related disasters and enhance local resilience. Broadly speaking, resilience can be thought of as a combination of the ability to withstand a negative shock and the subsequent speed of recovery (IPCC 2012). Here, we refer to these processes as *resistance*, i.e. the magnitude of the impacts, and *recovery*, which relates to reconstruction in the months following an event.

There is a strong demand for evidence-based policy advice in the aftermath of disasters. For instance, first responders need any indication possible on where to target the distribution of relief aid. In the longer term, it is of interest to study the extent to which additional aid is needed in order to facilitate reconstruction of homes and workplaces, and how to target this. If resistance and recovery are strongly dependent on initial wealth, it could, for instance, make sense to increase the coverage of existing poverty-based social protection systems, whereas if differences in resilience are mostly driven by a lack of access to services, it might be better to focus on re-building roads and other types of infrastructure.

This study outlines recent advances in the application of remote sensing data that could potentially improve relief assistance to cyclone-ridden urban areas. We ask: *When measuring cyclone impact, does it matter which method we use?* Secondly, *how important are neighbourhood characteristics for observed cyclone impact?* And finally, *what are the potentials and challenges of using satellite images to track the process of recovery from cyclone impacts?*

We contribute to the study of weather-related disasters in urban settings by outlining and discussing alternative ways of measuring both resistance to and recovery from tropical cyclones in urban areas. Furthermore, our focus on evidence at sub-neighbourhood level may contribute to improving targeting of both immediate relief aid and longer term social assistance.

The rest of the paper is organized as follows: in the next section, we outline a number of data sources and discuss their advantages and disadvantages. In Section 3, we analyze the magnitude and distribution of the damage caused by Cyclone Idai using different approaches. Section 4 investigates neighbourhood-level factors that influence resistance to cyclone damage, while Section 5 discusses the potential for using remote sensing data to track post-cyclone reconstruction.

## 2 Data sources

This section compares four types of data that can all be used to evaluate damage or the process of reconstruction following a cyclone: from on-ground assessments over analyses of satellite images with varying degrees of automation to fully automatic change detection on synthetic-aperture radar signals. While one could imagine several other ways of measuring cyclone impacts and resilience to these, the focus of this paper is the use of readily available satellite data. We include on-ground information as a point of reference.

## 2.1 On-ground information

Traditionally, the first overview of damage after a disaster like Cyclone Idai comes from in-situ reports by local or international aid agencies and first responders. Often, the United Nations Office for the Coordination of Humanitarian Affairs (UN OCHA) sets up an On-Site Operations Coordination Centre (OSOCC) at a strategic place, from where it coordinates relief efforts and publishes daily situation reports. In the days following a disaster, the information gathered at the OSOCC may come from a variety of sources: eye-witness reports, reconnaissance by car, and—when possible—footage from helicopter or drone flyovers. While all of this provides crucial quick information for search-and-rescue teams and distributors of assistance, the information is based on non-representative samples and will be biased, for instance by distance to the coordination centre or accessibility.

As time passes, a way of obtaining more solid on-ground information about the impacts of a disaster is to conduct a representative household survey. Ideally, there would be a pre-disaster baseline survey from which researchers can create a follow-up to study the same individuals over time. If well-timed and well-implemented, such a survey dataset could provide valuable in-depth information on impacts, coping mechanisms, and the process of recovery. Downsides to this type of data include the implementation costs, the time it takes to complete a survey, and the availability of a recent baseline sample.

For this study, one dataset with some of the above-mentioned characteristics was available, namely the latest round of the MUVA Urban Poverty Survey administered as part of the Inclusive Growth in Mozambique programme (IGM).<sup>1</sup> The sample includes around 1,000 individuals that were, among other things, asked about how the cyclone had affected their household. Among the variables included, interviewees could select among the following categories: *i) Home destroyed*, *ii) Family had to move*, *iii) Family business destroyed*, *iv) Family member died*, *v) Family member injured or ill*, *vi) Not affected at all*. Attached to all interviews are recordings of latitude and longitude, although as discussed below, their accuracy is questionable.

## 2.2 Manual inspection of aerial images

As commonly seen in the days following a major disaster event, the landfall of Idai prompted the United Nations Institute for Training and Research (UNITAR) to activate the so-called United Nations Operational Satellite Applications Programme (UNOSAT) Rapid Mapping Service. Using various satellite images, including commercial ones provided under the ‘International Charter: Space and Major Disasters’, workers at UNOSAT and REACH manually compared before- and after-images of the disaster zone to assess all damage to buildings (UNITAR 2019).

---

<sup>1</sup> <https://igmozambique.wider.unu.edu/>

Figure 1: Manual damage tags

(a) Google Earth, March 4, 2019



(b) Google Earth, March 26, 2019



Note: purple dots on the Google Earth images show a sample of the manual tags performed by UNITAR analysts. The building marked by a red square on the right side was missed in the tagging process.

Source: reproduced from Malmgren-Hansen et al. (2020), under the Creative Commons license [CC BY 4.0](https://creativecommons.org/licenses/by/4.0/).

The image data for manual marking of building damage include before-images from March 13 from GeoEye and after-images from March 26 from WorldView-2. The damage maps were gradually published from March 28 to April 4. Full coverage of the city of Beira was available 21 days after the cyclone made landfall in Beira. According to Malmgren-Hansen et al. (2020), the price of such a full tagging of a city like Beira lies in the order of US\$20,000–30,000 in total labour costs. An example of the tagged data can be seen in Figure 1. The maps are overall of high quality with both major and minor damage to buildings tagged. However, there are also errors, as illustrated by the red square on the right side, showing a building that was missed in the tagging process.

### 2.3 Automated analysis of high-resolution satellite images

Due to recent advances in computer vision methods, it is now possible to automatically detect and classify buildings on high-resolution satellite images (HRSI) using a convolutional neural network (CNN)

algorithm. For this study, satellite images have been downloaded via Google Maps application programming interface (API) every three to six months since late 2018. We apply the approach described in (Sohnesen et al. 2019) for processing the images and extracting variables on density and types of structures. A two-stage CNN was trained on the Fisker et al. (2020) dataset matched with satellite images to detect whether a sub-patch of 20x20m contains a building and if so, which of the classes *under construction*, *painted roof*, *grey roof*, or *non-residential* it belongs to. For presentation, the detection and classification have been aggregated to grid cells of 115x115m covering the entire city of Beira.

The images available here were downloaded in November 2018, June and September 2019, and January, April, and August 2020. Since the first available post-disaster satellite image was retrieved three months after the cyclone, these data were not highly relevant for measuring the immediate impacts. However, since buildings without roofs would be classified as *under construction*, and buildings with new roofs often belong to the *painted roof* category, it should be possible, in theory, to track the process of reconstruction taking place in the period June 2019 to August 2020. Section 5 includes a detailed discussion of the potentials and caveats of this method.

## 2.4 Changes in synthetic-aperture radar signals

In order to measure variation in the immediate impact of Cyclone Idai on local neighbourhoods in Beira, we draw on previous work focusing on the use of synthetic-aperture radar (SAR) signals from before and after the cyclone’s landfall. In particular, Malmgren-Hansen et al. (2020) find that satellite change detections from March 14 to March 20 or 26, 2019, is highly correlated in time with weather data from the cyclone impact. The data used for extracting change detections are from European Space Agency (ESA)’s Sentinel-1 synthetic-aperture radar sensor, which can take images regardless of weather conditions as opposed to optical satellite sensors. Change detections are derived from statistically comparing images at two time points, e.g. before and after the cyclone impact, to isolate the changes caused by that event. Furthermore, results showed that the immediate destruction and scattering of objects caused an increase in reflectivity while the subsequent clean-up period resulted in a (smaller) decrease in reflectivity. In this study, we employ the net increase in reflectivity from March 14 to March 26—i.e. destruction minus initial clean-up—instead of the binary change detection. Sentinel-1 images have a pixel size of 20m. It is therefore a significant change in an area of 20x20m that can be measured by Sentinel-1, as opposed to the commercial high resolution optical images that have a pixel size of 30x30cm in this case. Despite this, Malmgren-Hansen et al. (2020) are able to isolate changes caused on buildings by further filtering changes with a mask of building footprints drawn from OpenStreetMaps (OSM). The method is not completely independent of these unwanted changes but drastically reduces their influence on the results. The manually tagged damage is also filtered with a 1-metre radius to an OSM building footprint Malmgren-Hansen et al. (2020).

## 2.5 Comparison of data sources

The various data sources utilized in this paper have different advantages and disadvantages, and they are often used in different contexts for different purposes. Table 1 provides an overview of the different sources outlined above, in terms of the degree to which they can be automated, the time needed to generate information and results, the costs associated with undertaking the analysis, the level of detail in terms for spatial coverage, and finally what kind of analysis each data sources is often or usually suitable for.

The data sources are ordered according to perceived costs of implementation. In-situ surveys with reasonable coverage are seen as the most expensive option as they are very labour intensive and often require organization of several teams operating on the ground. Unlike the other sources that all rely on satellite data, in-situ household surveys can provide detailed information on households’ livelihood status as well as coping mechanisms and potential challenges. The satellite-based data sources have

advantages such as much higher spatial coverage, generally lower costs, and generally being easier to implement, especially in a situation during a cyclone like Idai. Among the satellite approaches, the SAR-based approach especially stands out as it does not depend on cloud-free images, and the data is available at no costs, while the two others (manual tags and CNN on HRSI) require cloud-free images, and there are costs associated with obtaining the images. In the latter’s favour is a higher resolution and likely accuracy.

Table 1: Data overview

	<b>In-situ surveys</b>	<b>Manual tags</b>	<b>CNN on HRSI</b>	<b>Change detection using SAR</b>
<b>Automation</b>	Very low	Low	High	Very high
<b>Time</b>	Weeks to months	Weeks to months	Weeks to months	Days
<b>Costs</b>	Very high	Medium	Medium	Very low
<b>Coverage</b>	Sample of households	All individual structures	All individual structures	All areas at 20x20 metres
<b>Purpose</b>	In-depth analysis of consequences	Targeting of rescue teams and relief aid	Targeting of humanitarian aid	Targeting of rescue teams and relief aid

Note: notes and comments here.

Source: authors’ elaboration.

### 3 Magnitude and distribution of impacts

The various sources of data available for assessing cyclone damage allow for a comparison and triangulation of the impact as measured by different data. This can shed light on the consistency between different data sources and lays the ground for assessing city-wide resistance to a disaster like Idai. In the following, we compare available data first at the structure level and afterwards at the neighbourhood level.

#### 3.1 Damage to individual structures

Two types of data assess damage at the structure level: household survey data (here the latest round of the MUVA dataset) as well as the manually tagged damage assessment from UNITAR (2019). Point locations (latitude and longitude) measured by survey enumerators can be difficult to link to a specific structure as GPS instruments often need to be taken outside for better connectivity. In combination with the inaccuracy of the technology, this typically results in several metres of error associated with the recorded GPS point. Figure 2 illustrates this, with many of the household reported GPS points being placed next to or between houses. Figure 2 also illustrates the differences in reported data from households and optical assessments from UNITAR. One house that is reported by households to have been totally destroyed is completely missed by the manual tagging of damages (a yellow house without a star), while another one that was tagged as damaged by the optical analysis reports no damage at all (a green house with a red star). Note that the green and yellow house tags in Figure 2 are a sample, while stars are supposed to cover all structures damaged. Hence, all the stars with no green or yellow houses do not indicate inconsistent reporting, only that the structure is not part of the MUVA sample. Among households that report that their homes being destroyed by Idai there is, on average, 11 metres between the GPS location of the house and the nearest structure with a manual optical tag. This is a large difference, indicating substantial difference in the indicators. It is worth mentioning that the MUVA data do not confirm that the interview took place at the structure that was destroyed. Thus, some of the discrepancy could be due to the household having relocated as a result of Idai.

Therefore, using survey data as a tool to identify severe cyclone damage at the level of individual buildings seems unfeasible. Even with modern GPS recordings, some degree of aggregation is needed, which again requires large sample sizes and representative sampling.

Figure 2: Damage assessment from optical analysis and household reports



Note: green houses report no damage from Idai, yellow total destruction; stars are manual tags based on optical images.

Source: authors' elaboration based on Google Maps, UNITAR, and MUVA data.

### 3.2 Assessment of damage at the neighbourhood level

Damage detected by radar data in Malmgren-Hansen et al. (2020) can be assessed in local areas, not individual structures. Hence, to make a comparison between the structure-level data in UNITAR (2019) and local area damage assessed by radar data, both data sources are aggregated up to grid cells of about 115x115m in Malmgren-Hansen et al. (2020). The two data sources build on two very different processes, each with advantages and disadvantages, but provide similar support for operational response to cyclones' damage. Though both measures are based on satellite data, the manual tags indicate damage of any severity, while SAR changes are more likely to only capture damage that is rather severe or a reflection of the damage to several houses. This reflects both the data-generating process and the higher resolution in the optical data used for manual tagging. When aggregated to the cell level, the severity of cyclone impact can be assessed by counting the number of tags within each grid cell, as illustrated in the heat maps in Figure 3. Image (a) shows that the most changes or damage detected by radar data are found along the eastern shore, but changes are generally found throughout the city. This is consistent with the direction of Idai that arrived from the east and hit the coastline first. Image (b) shows the count of manual tags based on manual tagging. As with change detection from radar, manually tagged damage is found throughout the city; but unlike change detection, the concentration of damage is higher in the western part of the city, further away from the coast. The higher concentration in those parts could reflect that these areas are more densely populated, leading to more individual tags.

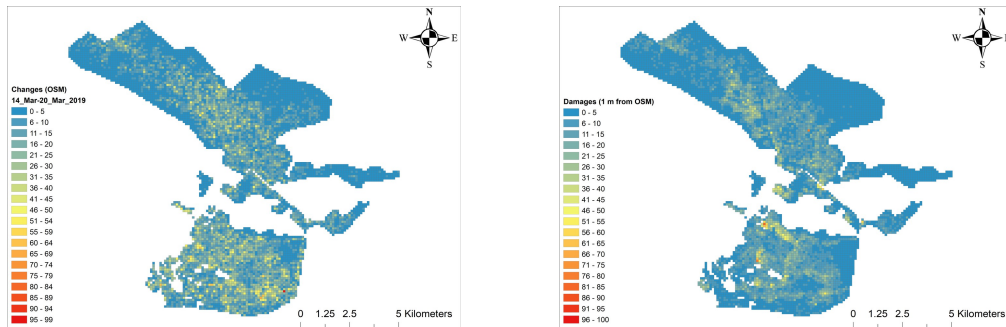
Manual tags and SAR changes have a spearman rank correlation of 0.55, and a Pearson correlation of 0.54 after square root transformation, corresponding to an explained variance score  $R^2 = 0.29$  (Malmgren-Hansen et al. 2020). This must be considered a low  $R^2$  and shows that the manual tags and radar-detected changes are two different sources of information on the cyclone's impact. One would expect that the manual tags catch smaller damages, while the radar data are more likely to capture larger damage. Fur-

ther, the manual tags are assessed between March 26 and April 4, while SAR changes are assessed on March 20, five days after the peak of the cyclone.

Figure 3: Cyclone impacts comparison

(a) Damage detected by radar data

(b) Manually tagged damages



Source: reproduced from Malmgren-Hansen et al. (2020), under the Creative Commons license CC BY 4.0.

#### 4 Neighbourhood resilience to cyclone impact

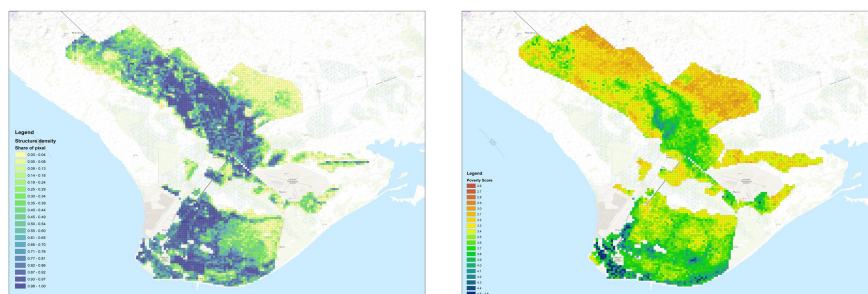
This section explores a number of factors related to neighbourhood-level resilience that could have affected the impact of Cyclone Idai across Beira. While looking at Figure 3, the cyclone damage seems evenly distributed across the urban area without any clear pattern. However, this might hide the fact that at the very local level, correlations could exist between impacts and prior conditions such as initial wealth, building density, and access to services.

Two sets of outcome variables that measure the immediate cyclone impact are considered in this section: i) changes in SAR recordings from a few hours before the cyclone to six and 12 days after, following Malmgren-Hansen et al. (2020), and ii) manual damage tags by UNOSAT between 11 and 21 days after the cyclone (UNITAR 2019). In terms of factors that might explain the net impact as observed in Figure 3, Figure 4 shows the distribution of two of them, namely structure density and initial wealth (measured by average proxy means test (PMT) score).

Figure 4: Sub-neighbourhood characteristics

(a) Structure density

(b) Estimated PMT scores



Source: authors' elaboration.

It is expected that there will be some variation in resistance to the damages caused by Cyclone Idai across the city and that this variation will be correlated with some, if not all, explanatory variables listed above. For instance, the homes of richer households are likely to be more resistant to strong winds due to better construction quality. This would in turn lead to fewer damage tags or lower increases in radar reflectivity. We also expect to see more resistance in denser areas and areas further away from the coast.

## 4.1 Estimation

In order to test the degree to which net cyclone impact is determined by pre-existing neighbourhood resilience, we merge data on initial wealth and building quantity and quality generated by Sohnesen et al. (2019) with that of cyclone damage developed by Malmgren-Hansen et al. (2020).

The analysis builds on a grid of cells of roughly 115x115m in size, with approximately 5,650 cells covering Beira. We estimate the following equation using Ordinary Least Squares (OLS):

$$Impact = \beta_1 initial.wealth + \beta_2 structure.density + \beta_3 dist.coast + \quad (1)$$

where *Impact* is either the detected increased reflectivity between March 14 and 26, or manual damage tags based on optical satellite images from March 13 and 26. The exact values relate to the share of pixels in a cell which show increased reflectivity or the number of damage tags divided by the number of building pixels. *initial.wealth* is the cell-level poverty score (a prediction of the average logarithm of consumption per capita) estimated by Sohnesen et al. (2019). This variable is approximately normally distributed around a mean of 3.4 and a standard deviation of 0.26. *density* is the share of a cell's area that is filled with structures. Wind speeds are likely to be stronger close to the shoreline, whereas the remaining areas of Beira will be partly sheltered by the coastal buildings. Therefore, *dist.coast* is log-transformed. Buildings in areas with higher structure density may also be more sheltered from the wind than less built-up areas.

## 4.2 Results

Below we outline the main results of estimating full and reduced versions of Equation 1 using OLS. Table 2 shows the relationships between resistance to Cyclone Idai and selected predictors using three different outcome measures at the cell level. Columns 1–3 use the share of pixels belonging to buildings with increased reflectivity between March 14 (right before the landfall of Idai) and March 26. Columns 4–6 use the number of manually tagged damages, based on visual inspection of optical satellite images on March 26, divided by the number of pixels belonging to buildings by cell.

Table 2: Cell-level cyclone resistance

	SAR Mar 14–26			Manual tags		
	(1)	(2)	(3)	(4)	(5)	(6)
Initial wealth	-0.09*** (0.01)	-0.05*** (0.01)	-0.08*** (0.01)	-0.10*** (0.01)	-0.11*** (0.01)	-0.08*** (0.01)
Density		-0.12*** (0.02)	-0.13*** (0.02)		0.03*** (0.01)	0.04*** (0.01)
Dist. coast			-0.01*** (0.00)			0.02*** (0.00)
Constant	0.74*** (0.01)	0.66*** (0.03)	0.88*** (0.06)	0.51*** (0.01)	0.53*** (0.02)	0.29*** (0.03)
N	5656	5650	5650	5005	5003	5003
r <sup>2</sup>	0.01	0.02	0.03	0.06	0.06	0.08

Note: standard errors in parentheses. \* p<0.10, \*\* p<0.05, \*\*\* p<0.01. Columns 1–3: share of building pixels with increase in reflectivity March 14–24. Columns 4–6: number of manual tags divided by number of building pixels March 14–20.

Source: authors' calculations based on Malmgren-Hansen et al. (2020) and UNITAR data.

Columns 1–3 focus on the increase in reflectivity in built-up areas from March 14 to 26. The 12-day time span is chosen so that the residents of Beira have had time to clean up fallen trees and other debris while

most of the damage to buildings would still be observable. Furthermore, any changes in radar signals caused by surface water are expected to play a minor role since this had mostly receded by March 26. In this specification, results are in line with our hypotheses. Richer areas are generally less affected by the immediate impact, and the same can be said of denser areas.

When looking at an alternative measure of cyclone impact, namely the number of damage tags recorded by UNOSAT based on images from March 26, similar correlations with initial wealth appear, while denser areas also seem to have more damage. The latter finding may be due to the fact that it might be easier to see physical damage to larger buildings than to smaller ones, or to a stronger focus on central areas of the city by the workers.

In summary, there is evidence to support the notion that richer areas are generally more resilient to cyclone damage than poorer ones. But the differences are generally not large: an increase in poverty score of one (equal to a move from the 5th to the 95th percentile of the wealth distribution) is only associated with an eight percentage point decrease in the share of pixels in a cell with damage. These differences are not substantial enough to warrant exclusion of ‘richer’ areas from rescue or relief aid efforts. However, in the case of Idai’s landfall on Beira, it should be noted that many of the richer areas are located closer to the coast and thus might have been exposed to stronger winds. On the other hand, inclusion of the distance to the coast does not alter the relationship between initial wealth and cyclone impacts.

## 5 Tracking post-cyclone rebuilding

The tracking of changes in structures on the ground over time has large potential for various use, especially in cities where informal and unplanned growth is common. Here, knowledge of such developments are often limited and city planners are often constantly struggling to keep up to date on current developments and needs. Frequent mapping of the growth and changes in use in different parts of the city could be an efficient tool assisting city planners. Similarly, such tracking could also be applied in the aftermath of a cyclone like Idai, showing which neighbourhoods are recovering faster and which ones might be lacking. Furthermore, such a massive destruction could lead to new investments that improve the quality of structures.

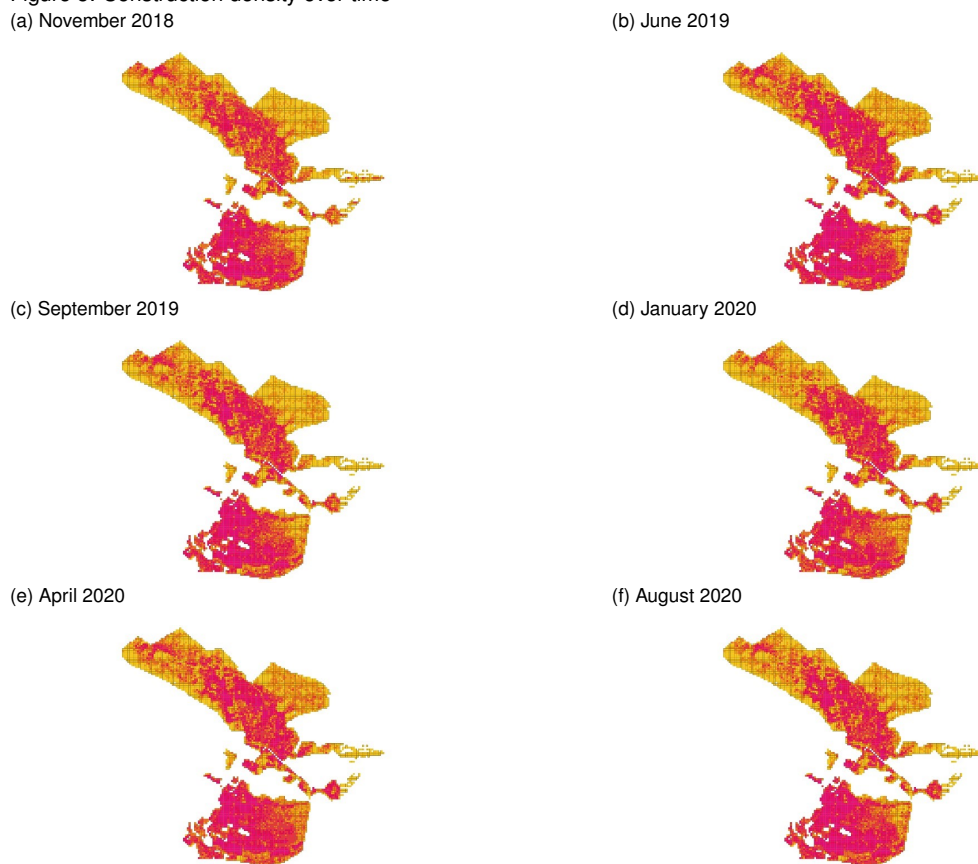
In Malmgren-Hansen et al. (2020), SAR change detection was used to map damage caused by Idai by statistically comparing pixels in SAR satellite images from two time points, one before and one after the cyclone. By isolating the SAR changes around the impact of the cyclone Idai with six days between the two time point, the authors in could map the changes primarily caused by the impact of Idai. Generally, SAR change detection has limited use in urban settings as the changes of interest are cluttered by the high activity in urban areas that would cause a SAR sensor to detect changes, such as a car being moved from one image to another. Due to this high level of urban activity and the fact that the SAR change detection method does not provide semantic information of the type of change, the method is not suitable for tracking long-term changes of urban development. Other methods exist for mapping urban settlements from SAR images, such as shown by Esch et al. (2012), though they do not provide as much information as high resolution optical satellite imagery.

The CNN approach developed in Sohnesen et al. (2019) is a tool that could provide such frequent tracking. Using images from Google’s API downloaded at six different points in time, the CNN detects structures and types of structures, providing evidence on rebuilding of Beira after the cyclone. The first images were downloaded in November 2018, before the cyclone, and the last images were downloaded in August 2020, 17 months after the cyclone. However, images from Google’s API do not come with metadata, including date of the image. Hence, before undertaking such an analysis, it is critical to know

if the images underpinning the analysis are updated frequently enough to provide a meaningful analysis of changes over time. An assessment of image updates—by pixel-wise subtracting images from each other—reveal that among the first three time periods (November 2019/June 2019; June 2019/September 2019; September 2019/January 2020) all images were updated. For the two last time periods (January 2020/April 2020; April 2020/August 2020) only 40 and 66 per cent of images were updated. Hence, some inertia in results should be expected due to lack of new images in some parts of the city for the two later time periods.

Figure 5 shows how structure density has developed over time according to the CNN detector. The figure shows a similar spatial distribution over time, though a closer inspection also reveals some areas that ‘flare up’ with more structures detected only in a single time period. This is unexpected as one would generally expect a more continuous development.

Figure 5: Construction density over time  
(a) November 2018



Source: authors' elaboration.

To ensure quality and robustness of results, a visual inspection of outliers in changes in construction density and type of structures between January and August 2020 was undertaken. The quality control revealed several examples of classical challenges in image detection, as well as some encouraging results for the CNN approach. The following key observations were found from the visual inspection of change outliers:

- **Seasonality** is a common problem in optical analysis as vegetation, especially tall trees, can hide structures part of the year. Figure 6 illustrates an example of this from this analysis, as roughly half of the structures are covered by trees in August but not in January. Adjusting the CNN detection algorithm to detect trees as a separate class did not solve the problem. Furthermore, the original training sample was from one point in time (Fisker et al. 2020), so the algorithm had not been exposed to different characteristics of structures at different points in time, which could cause a bias in detections.

- **Cloud coverage** is likely the largest source of uncertainty in optical remote sensing, which relies on the sunlight's reflection on ground for providing valid data. As seen on maps produced by the NASA Earth Observatory (n.d.), the Earth is heavily covered in clouds at any given moment with smaller probability over dry regions and higher over e.g. rainforest. A special challenge is semitransparent clouds, as these often are not detected by generic cloud removal algorithms that select images before they are published, while the semitransparent clouds can still hamper the data quality and significantly lower the level of information in an image. Figure 6 shows an example with one of the largest changes in construction density over six months, which is entirely caused by semitransparent clouds. The change in detected structures is clearly not driven by changes on the ground, but failure to detect buildings through the thin cloud layer.
- **Off-nadir imagery:** When buildings are observed from a satellite at nadir (directly under the satellite in the center of its field of view), they appear significantly different than under larger angles. Figure 7 shows this problem in the detection of structures, where the angle from which the structure is imaged changes its appearance substantially. The challenge is larger with taller structures, as more of the sides are imaged and they appear tilted. In Weir et al. (2019), the authors outline the problem of off-nadir imagery specifically in light of the challenges of building footprint detection.
- **Successful tracking of change:** Among the outliers of largest changes in construction density over the six months is also a true change. Figure 7 shows a positive result, where one of the largest increases in construction density between January and August 2020 is the rapid expansion of a new settlement.

Figure 6: Outliers caused by seasonality or cloud cover

**Seasonality**

(a) Construction density=0.16



(b) Construction density=0.03



**Cloud cover**

(c) Construction density=0.11



(d) Construction density=0.51



Source: Google Earth and authors' calculations.

Figure 7: Outliers caused by different angles or true rapid expansion

**Different image angles**

(a) Construction density=0.08



(b) Construction density=0.21



**True rapid expansion**

(c) Construction density=0.07



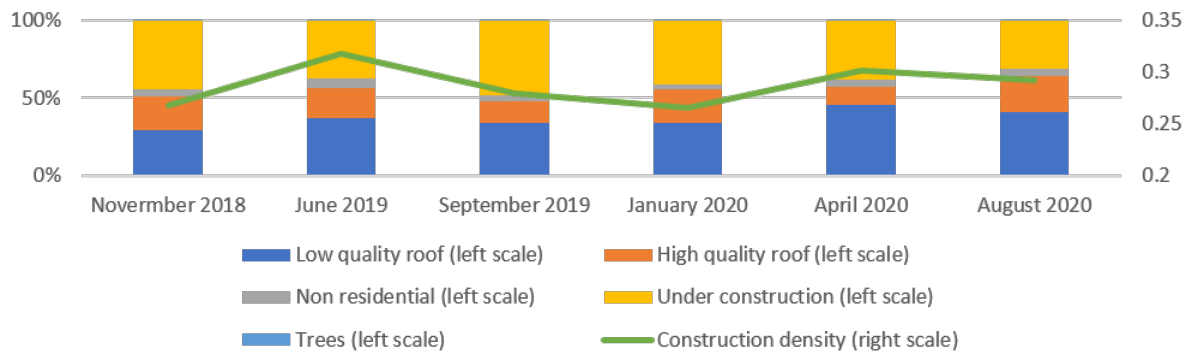
(d) Construction density=0.45



Source: Google Earth and authors' calculations.

The analysis of the changes in construction density (share of pixels identified as having a structure), as well as the distribution in types of structures, show an unexpected pattern (Figure 8). The first set of data after the cyclone (June 2019) show an increase in the number of structures, as well as an increase in the share of structures with low-quality roofs. Subsequent rounds of data seem to show a cyclical pattern following the year, as opposed to a trend, with more structure detections in fall/winter months (April to June) and fewer structures in summer months (November and January). This pattern over time is consistent with seasonality, indicating that the CNN detections of structures are biased, notably by tree coverage. The bias is so large in this case that it overshadows potential patterns of reconstruction after the cyclone. This questions the comparability over time, and the method's ability to truly track trends and the rebuilding of Beira. Hence, in the case of Beira—a city characterized by partial tree cover and seasonality—the attempt to track reconstruction in the months following Idai did not yield meaningful results.

Figure 8: Construction density over time



Source: authors' elaboration.

Though unsuccessful in this case, the use of CNNs to track the rebuilding of cities or the general growth of cities might still be feasible. Firstly, locations with less cloud cover and seasonality would be better suited. Secondly, an analysis over a longer time period and/or more observations would allow smoothing over time, which could remove/control for outliers and seasonality. Finally, the CNN approach developed in Sohnesen et al. (2019) contains specific drawbacks. i) The locations of houses were recorded in a survey in 2015, whereas the first images were downloaded in 2018. The delay was due to gap in funding. It is therefore assumed that not too many of the houses changed between the tagging of structures in 2015 and the training of the CNN based on images from 2018. ii) A well-known problem is the accuracy of the house locations, as the interviewers in the surveys do not make sure to stand close to the house when logging its position. As a result, some of the images that only contain part of a house or even no house at all are shown to the network during training. When training the CNN, it is assumed to be a small problem, though it does likely cause some uncertainty in the estimates. It is possible that higher quality datasets could improve this in future studies.

## 6 Concluding remarks

Measuring cyclone impacts—and resilience to cyclone impacts—is no easy task. This paper has compared four approaches to obtaining data in the aftermath of a major cyclone, three of which are derived from remote sensing. Taken separately, parts of the analysis provide strong results, showing great potential for use. Firstly, both manual tagging of optical images and radar data can be used to measure the immediate magnitude of impacts. The radar data from Sentinel-1 satellite can be used immediately and at low cost compared to the manual tags relying on cloud-free optical images and their processing. The success of the radar data depends, however, on the availability of building footprint data. In this case, it was available through OpenStreetMaps, while in other cases it might need to be generated first. Moreover, both approaches suffer from the lack of substantial validation of results. Such validation is difficult due to limited on-the-ground access, which is also why the satellite data is so attractive. The radar results are partly validated as the authors show that the detected changes coincide closely with weather data.

Secondly, it is shown that some pre-existing neighbourhood-level characteristics affected the severity of the impacts of Cyclone Idai. When analysed at the grid cell level (115x115m), initial wealth—as measured by a proxy for average household level consumption per capita—does have a statistically significant correlation with cyclone impacts, even when controlling for building density and distance to the coast. However, from a practical perspective, the differences seem to be negligible in the case of Beira.

Thirdly, the potential for measuring the longer-term process of reconstruction using high-resolution optical satellite imagery combined with convolutional neural networks is large, although so far unfulfilled. When analysing data from five different points in time up to one year and a half after Cyclone Idoi, random noise generally overshadows meaningful interpretation of changes in the measured quality and quantity of housing. An analysis of outliers exemplifies cases where seasonality, partial cloud cover, and different angles result in large fluctuations in the estimates. However, with more training data and better algorithms, this method could become a valuable source of information about post-disaster recovery in the near future.

## References

- Esch, T., Taubenböck, H., Roth, A., Heldens, W., Felbier, A., Schmidt, M., Mueller, A. A., Thiel, M., and Dech, S. W. (2012). 'TanDEM-X Mission-New Perspectives for the Inventory and Monitoring of Global Settlement Patterns'. *Journal of Applied Remote Sensing*, 6(1): 061702.
- Fisker, P., Malmgren-Hansen, D., and TP, T. S. (2020). 'TASIM: Tagged Structures in Mozambique'. Mendeley Data, V1. <https://doi.org/10.17632/pr8bgkj3c3.1>
- IPCC (2012). *Managing the Risks of Extreme Events and Disasters to Advance Climate Change Adaptation*. A Special Report of Working Groups I and II of the Intergovernmental Panel on Climate Change [Field, C.B., V. Barros, T.F. Stocker, D. Qin, D.J. Dokken, K.L. Ebi, M.D. Mastrandrea, K.J. Mach, G.-K. Plattner, S.K. Allen, M. Tignor, and P.M. Midgley (eds.)]. Cambridge, UK, and New York, NJ, USA: Cambridge University Press.
- Malmgren-Hansen, D., Sohnesen, T., Fisker, P., and Baez, J. (2020). 'Sentinel-1 change detection analysis for cyclone damage assessment in urban environments'. *Remote Sensing*, 12(15): 2409. <https://doi.org/10.3390/rs12152409>
- NASA Earth Observatory (n.d.). *Cloud fraction*. Available at: [https://earthobservatory.nasa.gov/global-maps/MODAL2\\_M\\_CLD\\_FR](https://earthobservatory.nasa.gov/global-maps/MODAL2_M_CLD_FR) (accessed April 2021)
- Sohnesen, T. P., Fisker, P., and Malmgren-Hansen, D. (2019). 'Using Satellite Data to Guide Urban Poverty Reduction'. Paper prepared for the IARIW-World Bank Conference, Washington, DC, November 7-8, 2019.
- UNITAR (2019). 'Damage Assessment in Neighborhood, in Cidade Da Beira, Sofala Province, Mozambique.'. Catalogue of maps: TC20190312MOZ. Available at: <https://unitar.org/maps/countries/67?page=0> (accessed April 2021)
- Weir, N., Lindenbaum, D., Bastidas, A., Etten, A. V., McPherson, S., Shermeyer, J., Kumar, V., and Tang, H. (2019). 'Spacenet mvoi: a multi-view overhead imagery dataset'. In *Proceedings of the IEEE/CVF international conference on computer vision* (pp. 992–1001).